South Carlsbad Boulevard Cliff Erosion Assessment Report

Submitted March 10, 2022

Summary

This study conducted coastal cliff retreat analysis to help inform the landward relocation of a segment of South Carlsbad Boulevard. The analysis consisted of a literature review, evaluation of cliff retreat from 1998 to 2020, and modeled 21st century future cliff positions Previous high resolution studies suggest historical mean cliff retreat rates range from 0.003-0.11 m/yr with maximum localized rates up to 0.66 m/yr. A new LiDAR survey was conducted in 2020 and used to measure cliff face retreat from 1998-2020 which ranged from about 0 to 0.47 m/yr with a mean of 0.039 m/yr. One section of cliff top retreated about 10 m between 2017 and 2020. Relatively high cliff steepening (increasing cliff top hazard) occurred from 1998-2020 between Terramar and Encinas Creek, compared to the South Carlsbad State Beach campground area.

Four existing predictive forecast cliff models were run for a sub region of the study near the Solamar Dr. intersection using the OPC (2018) 0.5% probability sea level rise scenario, USGS wave projections, and the 1998-2020 cliff retreat rates. In the forecast area, future cliff retreat of 10 m impacts the proposed project at the Solamar and Carlsbad Boulevard roundabout and a recreational trail. 10 m of retreat is lower than the 25th percentile for all four model outcomes. Present infrastructure in northern end of the forecast area becomes threatened under retreat scenarios with about 20 m of retreat, which is approximately the median retreat predicted from the combined model outcomes.

1.0 Introduction

In May 2020, the City of Carlsbad (City) was awarded funding by the California State Coastal Conservancy Climate Ready Program for the South Carlsbad Boulevard Climate Adaptation Project (Project) to develop managed retreat and long-term sea level rise adaptation options for a vulnerable stretch of coastal roadway. As a component of this project, the Scripps Institution of Oceanography Center for Climate Change Impacts and Adaptation was funded to conduct a detailed cliff retreat analysis to inform the landward relocation of a segment of South Carlsbad Boulevard. The following represents the results from this research and analysis endeavor.

2.0 Study Area & Forecast Area

The overall study area extends 4.6 kilometers (km) along the coast of Carlsbad, California, from the mouth of Batiquitos Lagoon at the south end of the study area to Terramar Point/Cerezo Bluffs (approximately Cerezo Drive) at the north end (Figure 1). The study area includes South Carlsbad State Campground and Las Encinas Creek area. Riprap currently exists near Las Encinas Creek outlet and at several beach access stairways within the study area (Figure 2). Schmidt hammer values, which provide an indication of rock hardness and uniaxial compressive strength (Katz et al., 2000), were taken at the cliff base (Young, 2018) and range from 0-16. Future cliff retreat rates were estimated for a portion of the study area (Forecast Area in Figure 1) specified by GHD (the consultant for this Project) and the City.

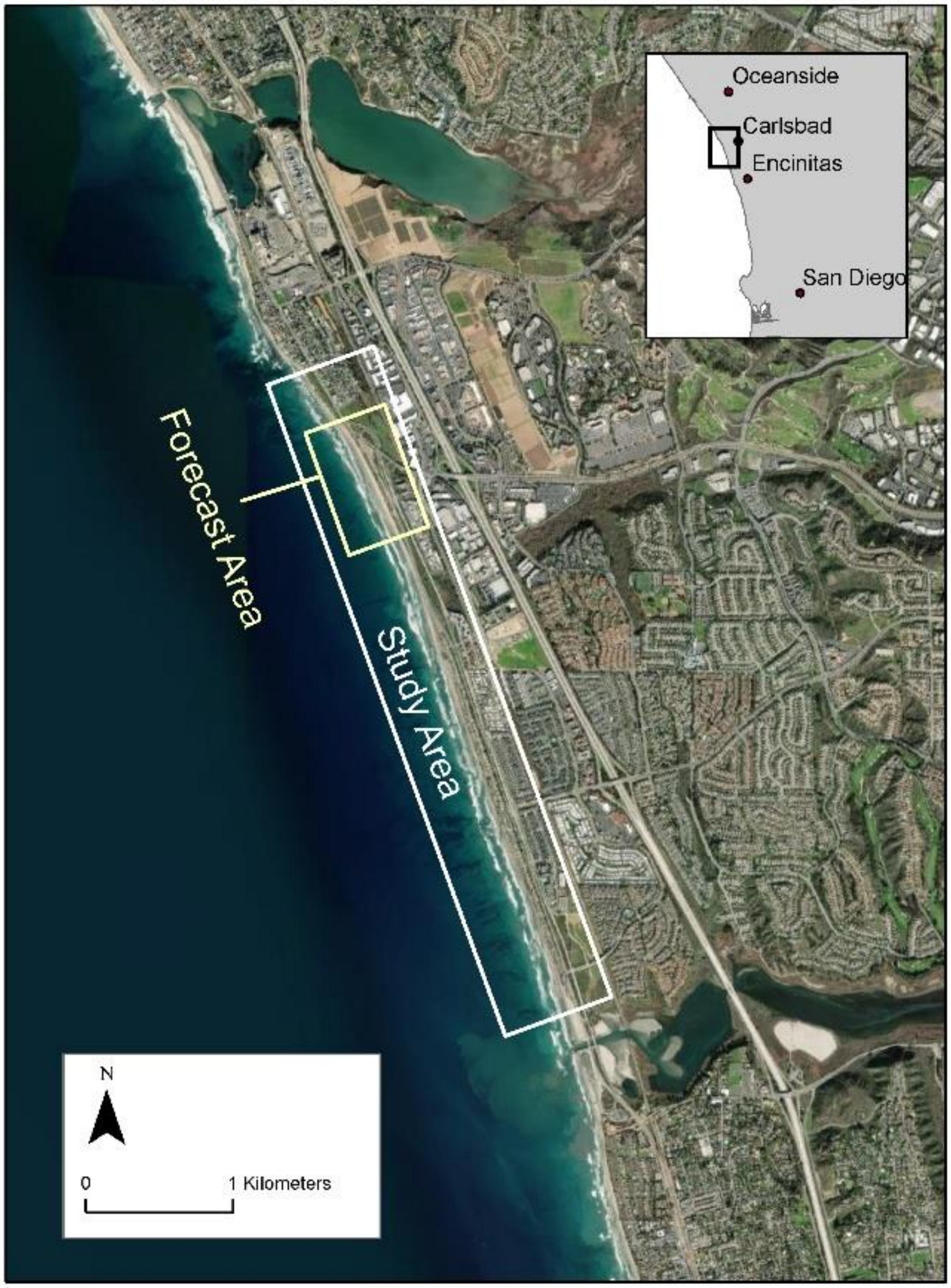

Figure 1. Study area map extending from approximately Batiquitos Lagoon to Terramar Point, and forecast area of estimated cliff retreat projections.

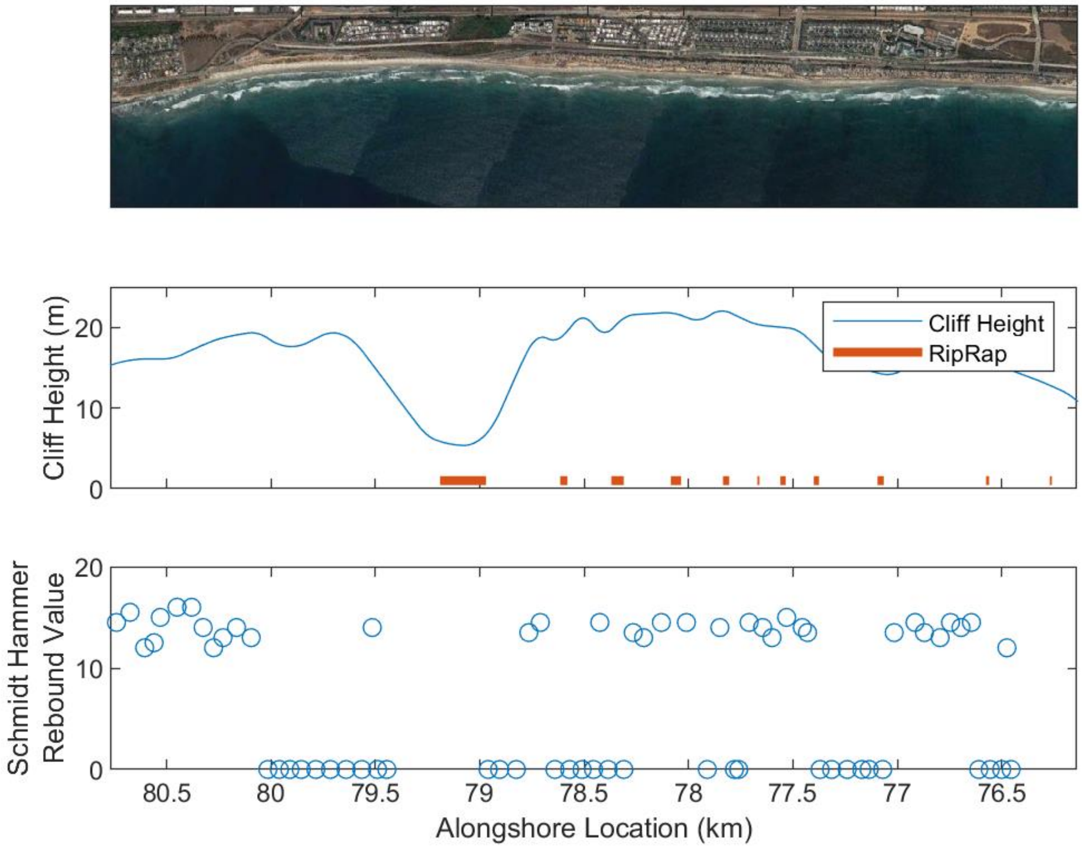

Figure 2. (Top) Aerial photograph of study area and (center) corresponding alongshore cliff height and riprap locations and (bottom) Schmidt hammer rebound values of rock hardness from Young (2018).

3.0 Previous Studies

Several studies have conducted cliff retreat analyses in the study area. Benumof and Griggs (1999) evaluated a 750 m segment in the South Carlsbad Campground using aerial photographs and estimated cliff top (Figure 3) retreat rates of 0.43 meters per year (m/yr) (standard deviation 0.08 m/yr) from 1956 to 1994. The collaborative study of Moore et al. (1999) reported cliff top retreat rates ranging from 0.03-0.58 m/yr for cliffs along South Carlsbad State Beach during the same time period. Using airborne light detection and ranging (LiDAR) data, Young and Ashford (2006) estimated cliff retreat rates averaged over the cliff face, from Batiquitos Lagoon to Oak Avenue, at 0.03-0.04 m/yr between 1998 and 2004.

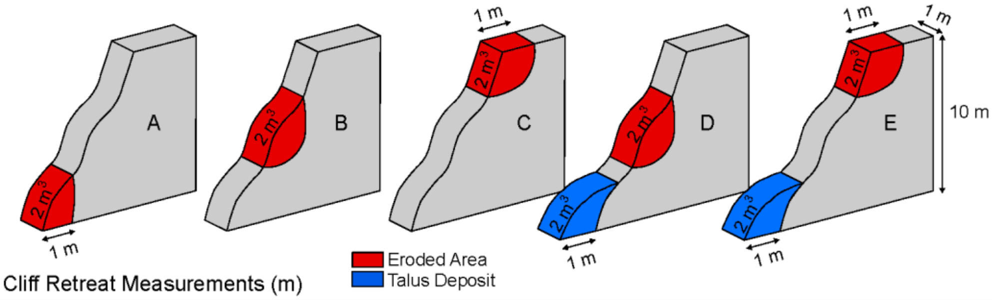

Cliff Retreat Measurements (m)

	A	B	C	D	E
Top =	0.0	0.0	1.0	0.0	1.0
Face (Erosion)=	0.2	0.2	0.2	0.2	0.2
Face (Deposition) =	0.0	0.0	0.0	-0.2	-0.2
Face (Net) =	0.2	0.2	0.2	0.0	0.0
Base =	1.0	0.0	0.0	-1.0	-1.0

Figure 3. Interpretations of idealized cliff changes and cliff retreat measurements. Figure modified from Young et al. 2009b.

Hapke et al. (2008; 2009) mapped cliff top retreat in the present study area using 1933 T-sheets (NOAA historic survey maps) and 1998 airborne LiDAR data on 130 shore-normal (perpendicular to the shoreline) transects spaced 20 m alongshore (with some gaps up to about 400 m). The mean and maximum cliff top retreat rates for these transects were 0.06 m/yr and 0.21 m/yr, respectively, with estimated errors of 0.20 m/yr.

Young (2018) resampled the Hapke et al. (2008) 1933 and 1998 cliff top edge lines at a higher 5 m alongshore resolution and found mean retreat rates of 0.06 m/yr (Table 1, Figure 4). Young (2018) also used airborne LiDAR datasets to measure cliff change from 1998 to 2009 at 5 m alongshore resolution and found mean cliff top and face retreat rates of 0.11 and 0.04 m/yr, with some cliff top locations exceeding 0.40 m/yr. Recently, Swirad and Young (2021) used airborne LiDAR from 2009 and 2016 and automated procedures to estimate mean cliff top and face retreat rates of 0.003 and 0.05 m/yr, respectively.

Young et al. (2009a) used airborne LiDAR datasets and measured cliff face volume changes between 2002-2006 ranging from 0 to ~2 m^3/m/yr.

Overall, historical mean cliff top and cliff face retreat estimates for high-resolution studies in the study area range from 0.003-0.11 and 0.04-0.05 m/yr, respectively. The rates vary between these previous studies because of variability in the original data sources, differences in mapping resolution, methods, time periods analyzed, and actual differences in erosion rates and processes.

Table 1. Summary of retreat rates from previous studies with high-resolution coverage in the study area.

	Cliff Top Retreat Rate (m/yr)			**Cliff Face Retreat Rate (m/yr)**	
Study	Young (2018)	Young (2018)	Swirad and Young (2021)	Young (2018)	Swirad and Young (2021)
Time Period	1933-1998	1998-2009	2009-2016	1998-2009	2009-2016
Maximum	0.22	0.42	0.13	0.25	0.66
Mean	0.06	0.11	0.003	0.04	0.05
Minimum	0.00	0.01	0.00	0.00	0.00
Standard Deviation	0.04	0.07	0.02	0.04	0.08

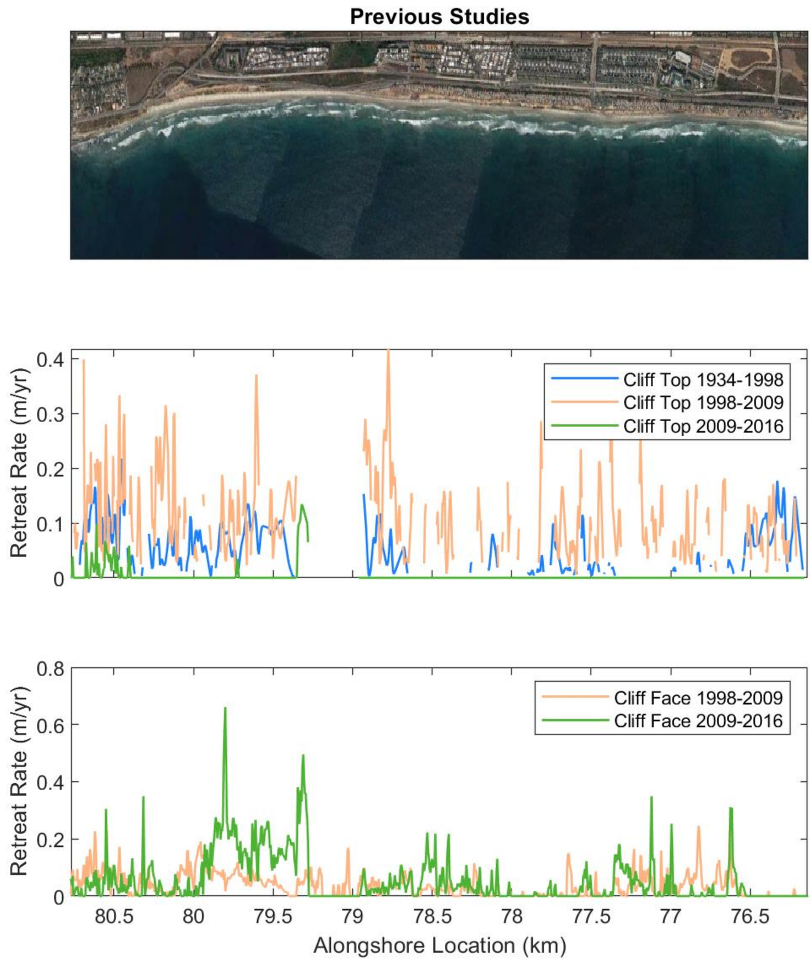

Figure 4. (top) Aerial image of study area and (center) corresponding alongshore cliff top retreat rates from previous high-resolution studies (Young, 2018; Swirad and Young, 2021), and (bottom) mean cliff face retreat rates from previous high-resolution studies (Young, 2018; Swirad and Young, 2021).

In 2017, the City of Carlsbad prepared a Sea Level Rise Vulnerability Assessment (City of Carlsbad, 2017) using cliff erosion projections for the Project study area (Figure 5) based on the United States Geological Survey (USGS) Coastal Storm Modeling System - CoSMoS 3.0 for Southern California (Barnard et al., 2018). The CoSMoS 3.0 modeling approach estimated bluff edge erosion using a baseline bluff top edge established from a 2010 digital elevation model. CoSMoS projections are based on historical erosion rates from 1933 to 1998 developed for the USGS National Shoreline Assessment (Hapke et al. 2008). The Sea Level Rise Vulnerability Assessment (City of Carlsbad, 2017) used sea level rise scenarios of 1.6 ft (0.5 m) and 6.6 ft (2.0m).

Figure 5. Map of potentially vulnerable parcels in Carlsbad with projected 2050 sea level rise of 1.6 ft and associated bluff retreat (Figure 6 in City of Carlsbad (2017)).

The USGS CoSMoS projections were updated in 2018 to CoSMoS 3.0 Phase 2 (Barnard et al., 2018) and show retreat rates from 2010-2100 and provide estimated future retreat for a range of sea level rise scenarios up to 5 m. For the transects in the Project's forecast area (Table 2), CoSMoS estimates cliff retreat of 0.06-0.12 m/yr for 1 m of sea level rise. CoSMoS 3.0 Phase 2 data are available for viewing using Our Coast Our Future online map viewer (https://ourcoastourfuture.org/, Figure 6).

Table 2. CoSMoS 3.0 Phase 2 Cliff Retreat rates for the forecast area.

	Cosmos Transect	805	806	807	808	809	810	811	812	813
	Cosmos Historical Retreat Rate (m/yr)									
		0.04	0.05	0.08	0.06	0.06	0.04	0.05	0.06	0.06
	Cosmos Projected Retreat Rate (m/yr)									
Sea Level Rise Scenario (m)	**0.25**	0.05	0.06	0.07	0.05	0.06	0.08	0.06	0.06	0.06
	0.5	0.05	0.07	0.09	0.06	0.07	0.08	0.07	0.08	0.07
	0.75	0.06	0.08	0.11	0.07	0.08	0.08	0.08	0.09	0.08
	1	0.06	0.09	0.12	0.08	0.09	0.1	0.09	0.1	0.09
	1.25	0.08	0.11	0.14	0.1	0.1	0.11	0.11	0.12	0.1
	1.5	0.1	0.13	0.17	0.12	0.12	0.13	0.13	0.14	0.12
	1.75	0.11	0.14	0.18	0.13	0.13	0.14	0.14	0.16	0.14
	2	0.14	0.17	0.2	0.14	0.16	0.16	0.15	0.18	0.16
	5	0.34	0.38	0.45	0.38	0.29	0.37	0.38	0.26	0.26
	Uncertainty	0.15	0.15	0.15	0.15	0.15	0.15	0.15	0.15	0.15

Figure 6. Example CoSMoS 3.0 Phase 2 projected cliff retreat for 2.5 ft (0.75 m), 3.3 ft (1 m), and 6.6 ft (2.0 m) of sea level rise within the study area (source: Our Coast Our Future online viewer). Red is the zone of cliff retreat.

4.0 Evaluation of Existing Condidtions

To assess existing conditions, a combined drone and mobile terrestrial LiDAR survey was conducted on September 17, 2020 (Figure 7). The drone and terrestrial surveys were merged to provide complete coverage in complex topographic areas, such as the northern section of the study area where sea caves and notches are common.

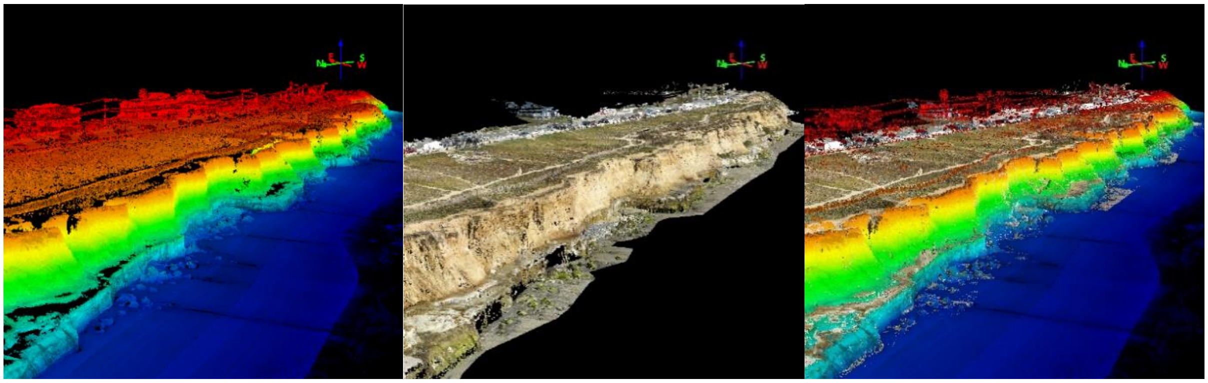

Figure 7. LiDAR data collected on Sep 17, 2020 from (left) a ground based mobile LiDAR system, (center) a drone based LiDAR system, and (right) the combined LiDAR data, used to provide complete surface coverage.

The most northern portion of the study area (Figure 8) contains numerous hazardous sea caves, notches, and bluff overhangs. As these features erode farther into the cliff, the likelihood of cliff failure increases. The depth of these over-vertical features on the lower and upper cliff were mapped using the recent 2020 LiDAR survey (Figure 8). These features can fail catastrophically and cause significant cliff top retreat, as evidenced by a collapse with 9 m of retreat shown in Figure 9 section P3.

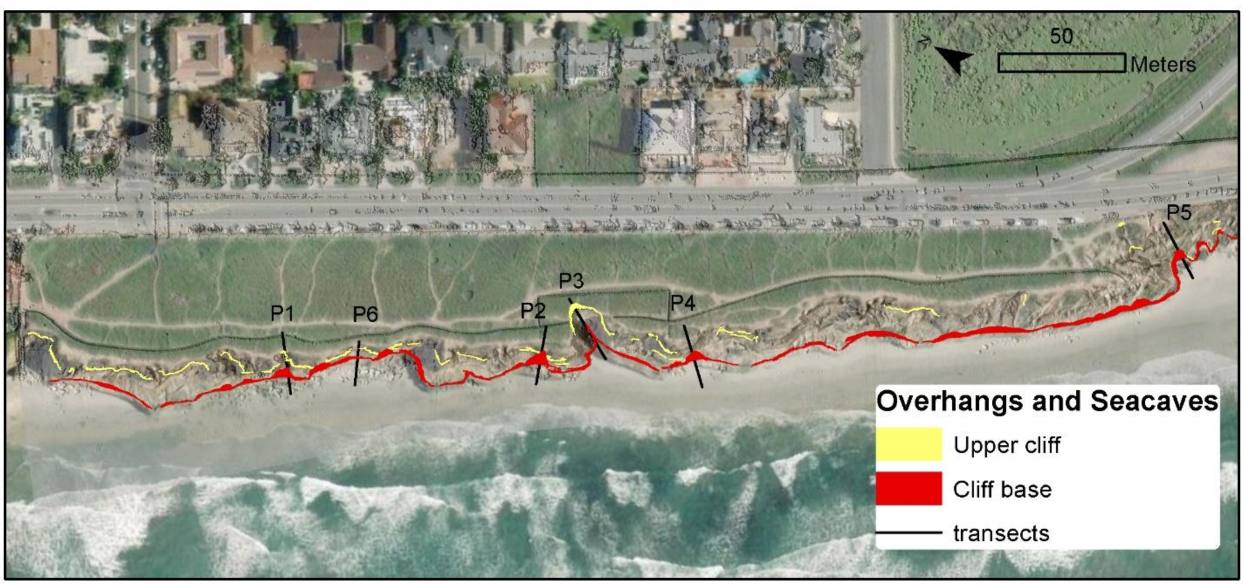

Figure 8. Areas with over-vertical topography in the upper and lower cliff obtained from a Sept. 17, 2020 LiDAR survey combined from drone- and truck-based mobile LiDAR systems. Labeled cross shore transects are shown in Figure 9.

The northern portion of the study area (Figure 8) was also inspected to evaluate recent changes by comparing a 2017 LiDAR survey to the recent 2020 data at specific cross shore profiles. Changes include lower cliff cantilever block failures at transects P1, P2, P4, and P5, a significant upper cliff failure that included ~10 m of retreat at P3, and a few meters of retreat across most of the cliff profile at P6. P2 changes observed at the cliff base could be from new notch development or changes in beach profiles inside the notch during the 2017 survey.

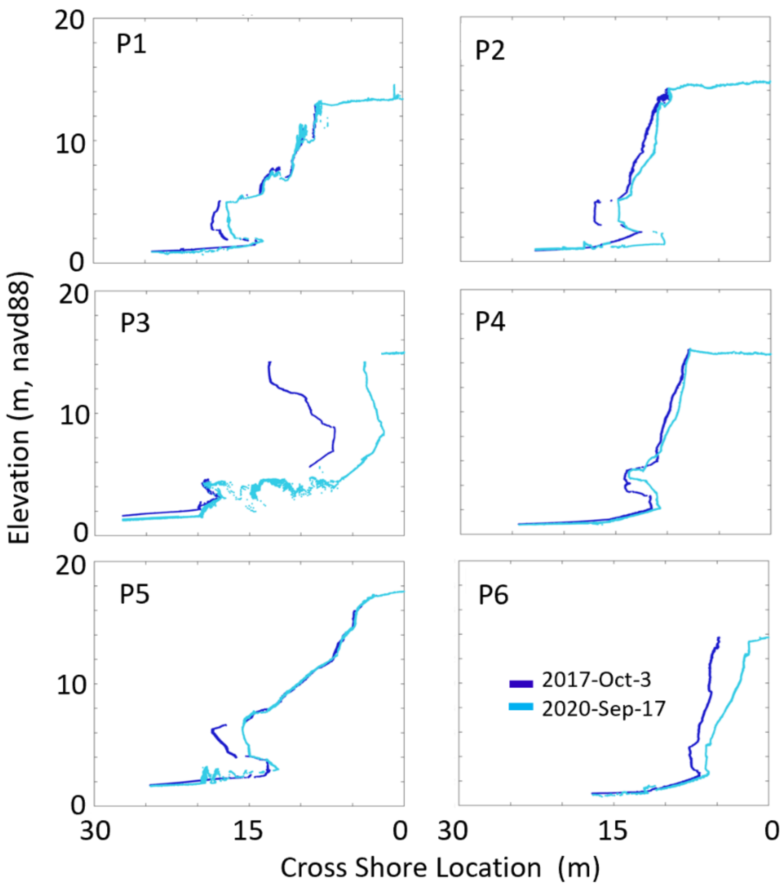

Figure 9. Selected cliff profiles (with the ocean to the left in each plot) in the northern portion of the study area showing significant changes between 2017 and 2020, including about 10 m of cliff top retreat at profile P3. Transect locations are shown in Figure 8.

5.0 Evaluation of Cliff Change 1998-2020

The new 2020 LiDAR dataset was used to evaluate cliff change from 1998 to 2020 to capture the longest time span of available high-resolution LiDAR data. Cliff top, cliff face, and cliff base retreat rates were evaluated at 5 m alongshore resolution (Figure 10) and provide change metrics on 3 different portions of the cliff. Cliff top and base positions were evaluated initially using cross shore profiles combined with automated detection methods (Swirad and Young, in review) and then visually inspected and edited.

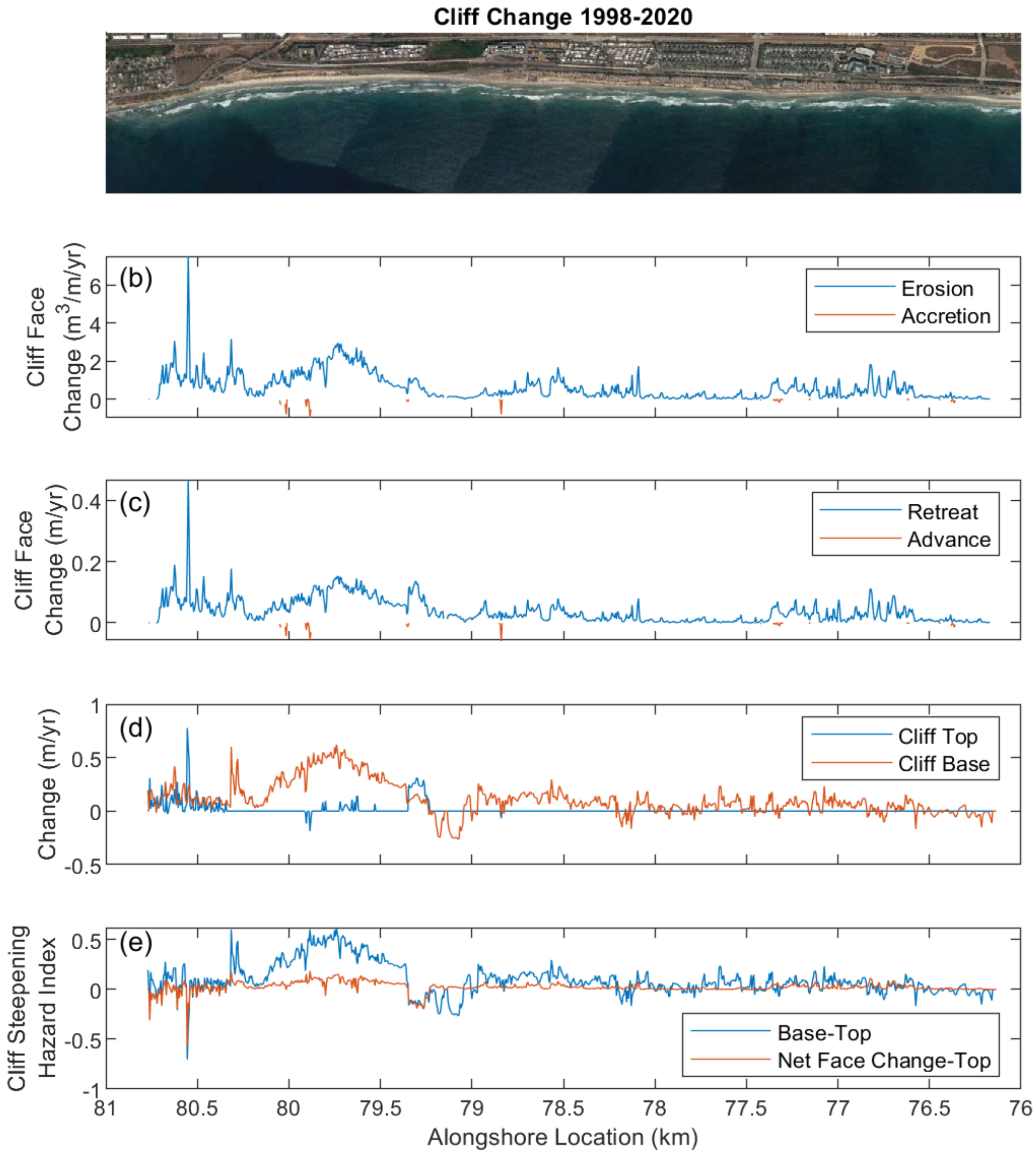

Figure 10. Cliff changes between 1998 and 2020 showing (b) volumetric change rate, (c) cliff face averaged retreat rates, (d) cliff top and cliff base change rates, and (e) a cliff steeping hazard index computed as the difference between lower and upper cliff changes. Higher values represent overall cliff steepening and increased cliff top retreat potential.

To evaluate overall vertical changes (Figures 10 and 11) and cliff face retreat rates from 1998-2020 (Figure 10) LiDAR point data were processed into 0.5-m resolution digital elevation models using the last return (if multiple returns were available) and a natural neighbors technique (Sibson, 1981). Digital change grids, estimated by differencing successive digital elevation models created using these LiDAR datasets, show both negative (erosion) and positive (accretion, talus deposits) changes. Sources of digital change grid error include the basic LiDAR observations, spatial interpolation, and vegetation. Elevation changes can indicate landslide motion, land erosion, talus deposition, topographic beach changes, and anthropogenic changes.

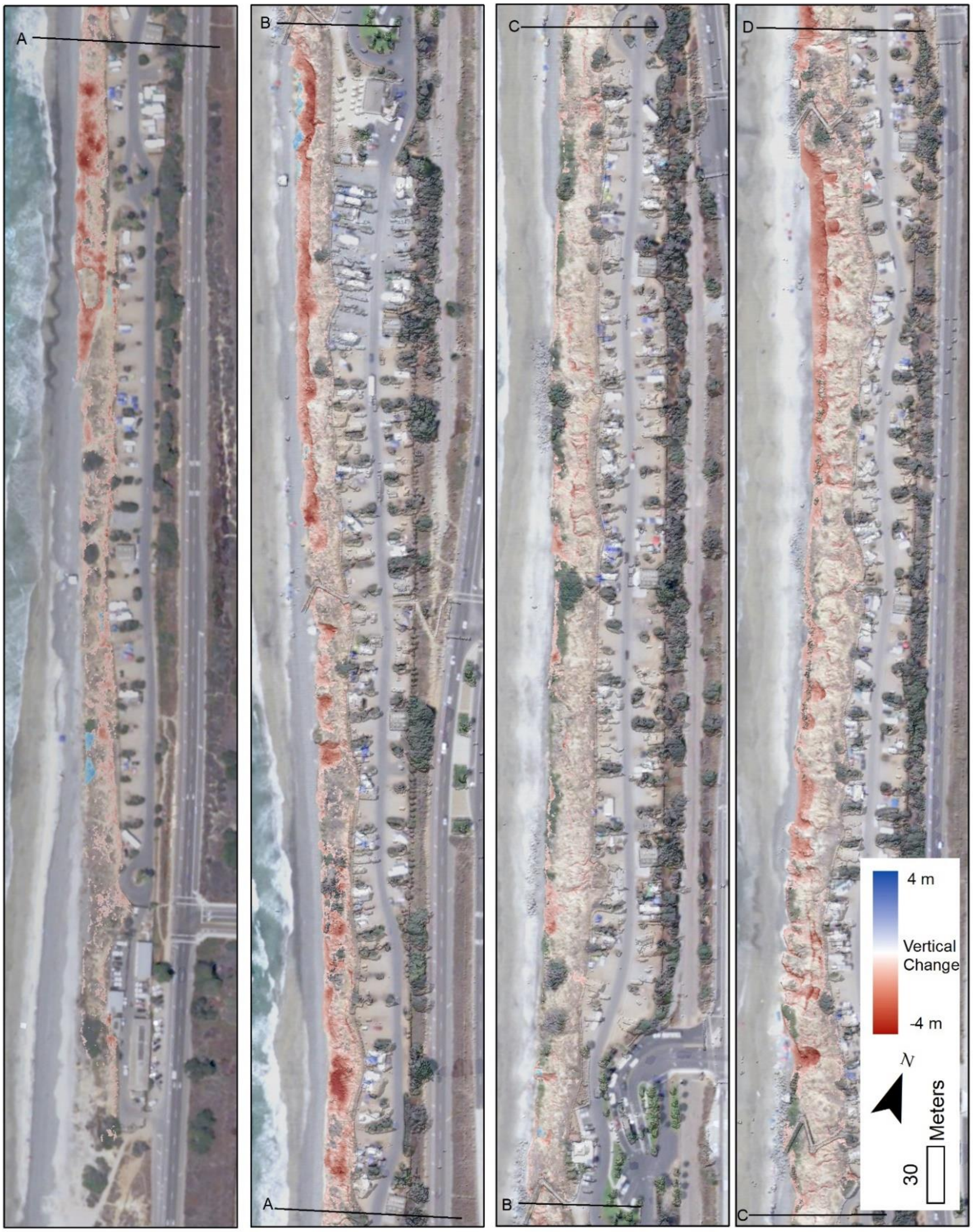

Figure 11. Vertical change maps of the south portion of the study area, spanning the South Carlsbad State Beach Campground, showing erosion (red) and deposition (blue) between 1998 and 2020. Colors saturate at +/- 4 m. From left to right, the panels go northward. Matchlines between panels and Figure 12 are indicated.

Figure 12. Vertical change maps of the north portion of the study showing erosion (red) and deposition (blue) between 1998 and 2020. Colors saturate at +/- 4 m. From left to right, the panels go northward. Matchlines between panels and Figure 11 are indicated.

Changes were separated into negative (i.e. cliff erosion) and positive (i.e. talus deposits) volumetric changes and then evaluated in 5 m wide (in the alongshore direction) compartments. Dividing the volumetric compartment changes by the cliff height and compartment width (5 m) yielded bulk negative and positive cliff face changes, equivalent to average cliff retreat/advance over the cliff face (Figure 10). Cliff heights were obtained from the digital elevation model. The cliff face retreat from 1998-2020 ranged from about 0 to 0.47 m/yr with a mean of 0.039 m/yr.

Cliff retreat measures on different parts of the cliff can differ substantially and provide information on geomorphic change and relative cliff top stability. Cliff top retreat reduces the overall cliff slope, while cliff base and cliff face erosion (not concentrated at the cliff top) cause slope steepening, thus reducing overall cliff stability. Young et al. (2009b) suggested the difference between cliff top and cliff face erosion could be used as a cliff top retreat hazard index (Figure 13). For example, as the cliff face retreat exceeds cliff top retreat, the cliff becomes more unstable, and vice versa. A cliff steepening hazard index, defined here as the cliff base or cliff face retreat minus the cliff top retreat, increases with overall cliff steepening. Positive hazard values indicate the cliff face or base retreat rates exceed the cliff top retreat rates, suggesting a higher relative potential for future cliff top failure. Based on cliff retreat rates from 1998-2020, relatively high cliff top hazard indexes exist in the northern portion of the study area between Terramar and Las Encinas Creek, compared to the South Carlsbad State Beach Campground area (Figure 10e).

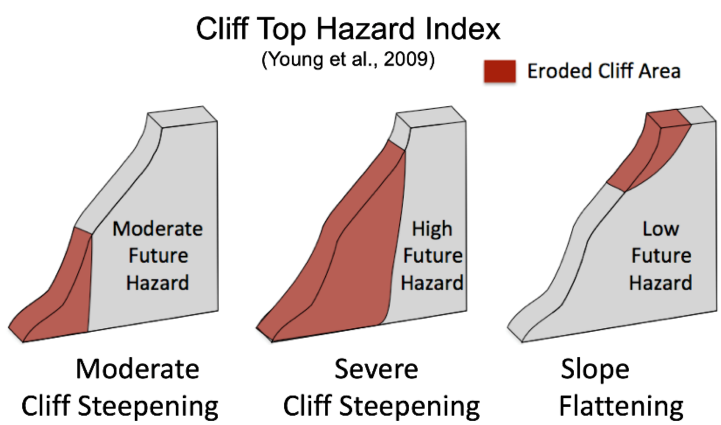

Figure 13. Conceptual cliff changes showing the cliff top hazard index developed by Young et al. (2009b). Profiles with more erosion on the lower and middle cliff cause overall cliff steepening and an increase in the cliff top hazard index.

6.0 Cliff Retreat Projections

Cliff retreat projections are limited to a 940 m section in the Solamar area, extending from the north end of Las Encinas Creek riprap to approximalely the intersection of Palomar Airport Road and Carlsbad Boulveard, approximately (Figure 1).

6.1 Model Introduction

This study estimated future cliff retreat (e.g. landward movement of cliff-base positions) of Carlsbad cliffs using four coastal cliff evolution models adapted from the existing scientific literature: modified Brunn (Bray and Hooke, 1997), modified SCAPE (Walkden and Dickson, 2008; Ashton et al., 2011), Trenhaile-Lite (Trenhaile, 2000; Limber et al., 2018), and Energy-Flux (Limber et al., 2018). All four models assume cliff erosion is primarily driven by wave action and iteratively calculate annual changes of the cross-shore profile of a cliff and fronting beach system. Other potentially important erosion factors such as rainfall (e.g. Young et al., 2009a; 2021) and groundwater are not specifically modeled but are implicitly included in the historical cliff retreat rates used to calibrate and run the models. For each iteration, the Trenhaile-Lite and Energy-Flux models update the whole cross-shore profile based on the amount of wave energy available at the cliff base and resulting cliff retreat, which subsequently influences wave transformation across the fronting beach and cliff retreat in the next iteration. Therefore, these two models work in a feedback system. On the contrary, the modified Bruun and modified SCAPE models only iteratively calculate the cliff base positions, without considering changes in the model cross-shore profile from previous time steps.

The modified Bruun and modified SCAPE models assume future cliff retreat ($R2$) depends on historical cliff retreat ($R1$), and historical ($S1$) and future ($S2$) sea level rise. The modified Bruun model is also influenced by profile geometry, closure depth (most landward depth with no significant bathymetric elevation change), and back shore geologic composition.

The models are expressed as:

$$R2 = R1 + (S2 - S1)\left(\frac{L}{P(B+h)}\right) \qquad \text{(Eq. 1, Modified Bruun)}$$

$$R2 = R1\sqrt{S2/S1} \qquad \text{(Eq. 2, Modified SCAPE)}$$

where L, B, h, and P in Eq. 1 are the cross-shore length of the active profile (L), cliff height (B), closure depth (h), and the proportion of sediment eroded that is sufficiently coarse to remain within the equilibrium shore profile (P), respectively.

The modified Bruun model is adapted from the widely used Bruun rule for sandy beaches (e.g. Bruun, 1962), which assumes conservation of sediment and an equilibrium profile shape and is the most basic of the four models used here. The modified SCAPE model is expressed as a relatively simple relationship (Eq. 2), but was derived from detailed process-based modeling of soft cliff coasts using the full SCAPE model version (Soft Cliff And Platform Erosion, Walkden and Dickson, 2008). Therefore, the modified SCAPE (Eq. 2) model is considered more physics-based compared to the modified Bruun model (Eq. 1), even though both models have relatively simple mathematical expressions.

The Trenhaile-Lite and Energy Flux models further assume that, in addition to historical cliff retreat (*R*1), and historical (*S*1) and future (*S*2) sea level rise, future cliff retreat (*R*2) also depends on wave energy transformation across surf and swash zones and, therefore, the slope of the beach fronting the cliff. In both models, the beach slope is defined as the linear slope from the cliff base at mean sea level and the wave breaking point, where the water depth equals $H_b/0.78$ (H_b: breaker height) (Battjes, 1974).

The wave force available for cliff erosion is calculated as follows:

$$F_w = \rho \frac{H_b}{1.56} e^{-xw} \quad \text{(Eq. 3, Trenhaile-Lite)}$$

$$F_w = \left(\frac{1}{8}\rho g H_b^2 \sqrt{\frac{gH_b}{0.78}}\right) e^{-xw} \quad \text{(Eq. 4, Energy Flux)}$$

where ρ, g, and x are the density of water (1025.2 kg/m^3), gravitational acceleration (9.8 m/s^2), and a decay constant (0.05 m^{-1}, Limber et al., 2018) that represents the dissipation of wave energy across the surf and swash zones, respectively. w is the width of the surf and swash zones and is calculated as follows:

$$w = \frac{H_b/0.78}{\tan\alpha} \quad \text{(Eq. 5)}$$

where α is the beach slope. The future cliff retreat (*R*2) in each iteration is estimated as follows:

$$R2 = K \cdot F_{w-total} \quad \text{(Eq. 6)}$$

where *K* is a calibration coefficient that converts wave energy available at a model cliff base to cliff retreat distance. $F_{w-total}$ is a measure of annual wave forcing (kg/m^2 for Trenhaile-Lite, and kg m/s^3 for Energy-Flux) calculated using a time series of wave data at a given site.

6.2 Model calibration (2000-2020)

Calibration of the Trenhaile-Lite and Energy-Flux models used modeled historical hindcast wave data, observed historical cliff retreat data (*R*1), and observed sea level rise data (*S*1) between 2000 and 2020. The observed historical sea level rise rate at the La Jolla station (~ 28 km south of the study site) was 2.13 mm/yr (Figure 14, tidesandcurrents.noaa.gov, station 9410230).

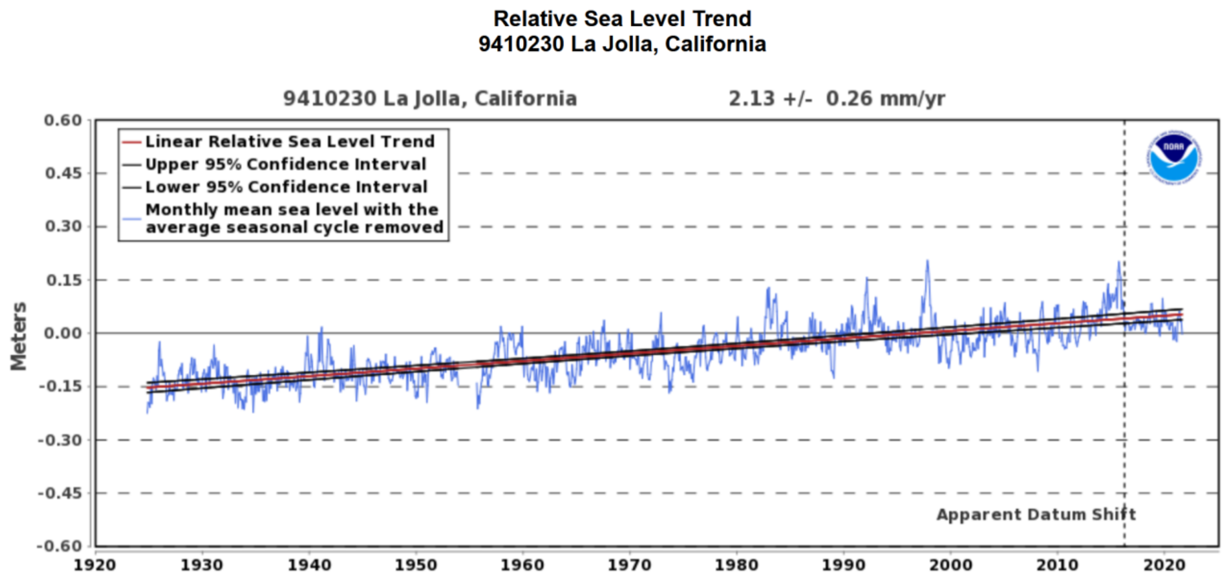

Figure 14. Relative observed sea level trends in La Jolla, CA (https://tidesandcurrents.noaa.gov/sltrends/sltrends_station.shtml?id=9410230).

The calibration coefficient (*K*) relates the historical cliff retreat rate to historical wave force as follows:

$$K = \overline{R1} / \bar{F}_{w-total} \quad \text{(Eq. 7)}$$

where $\bar{F}_{w-total}$ is the mean annual wave force over the 2000-2020 time period, and $\overline{R1}$ is the mean observed historical cliff retreat rate during the same period (Fig. 14a, in total 196 cases). The observed historical cliff face retreat rates from 1998-2020, evaluated in Section 5, were assumed to represent years 2000-2020 and ranged from 0.006-0.18 m/yr with a mean and median retreat of 0.076 and 0.071 m/yr, respectively.

Hourly 2000-2020 hindcast wave data (Figure 15b) was estimated using a buoy-driven regional wave model (O'Reilly et al., 2016), and converted to three-hour average wave data consistent with the USGS projected wave data (Hegermiller et al., 2016) used for model prediction. The calibration run was initiated with a simplified cross-shore profile (Figure 15c) based on 2009-

2011 LiDAR observations (2013 NOAA Coastal California TopoBathy Merge Project). No calibration was done for the modified Bruun and modified SCAPE models because both models are insensitive to wave conditions.

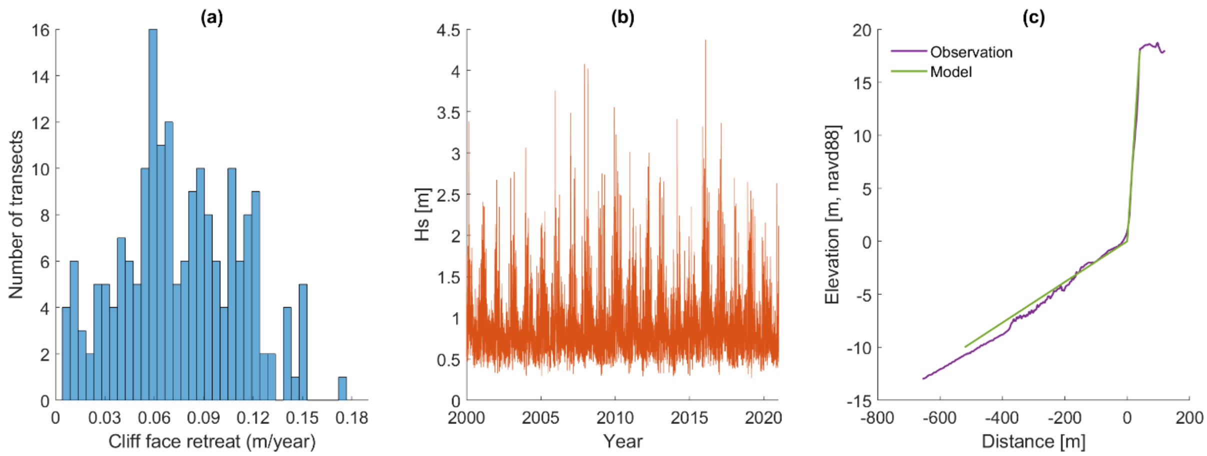

Figure 15. (a) Observed mean cliff retreat rate between 1998-2020, (b) modeled nearshore significant wave height (Hs), and (c) observed and simplified cross-shore profile used for the modeling.

6.3 Model prediction (2012-2100)

Model runs were conducted for the Ocean Protection Council (OPC) (2018) 0.5% probability La Jolla sea level rise scenario with specified water levels of 0.63 m in 2050, 1.10 m in 2070, and 2.16 m in 2100[1]. All model runs used a one-year time step. A quadratic function fit to the specified OPC (2018) water levels was used to estimate sea levels between 2012 and 2100 (Figure 16a). The simplified cross-shore profile (Figure 15c) was used to represent the forecast area.

The modified Bruun model runs used geometric parameters of the simplified observed cross-shore profile (Figure, 14c; Table 3) and measured cliff sand content of (P=0.9, Young et al., 2010). The closure depth was estimated at 8 m (Birkemeier et al., 2012). The *h* model parameter was modified to 9.5 m to account for the cliff base elevation (1.5 m) and to maintain consistency with the geometric relationships of the modified Bruun model.

For Trenhaile-Lite and Energy-Flux model runs, the future cliff retreat (*R*2) of a given year was estimated using the projected wave data (a time series of three-hour average wave data from USGS (Hegermiller, et al. 2016); Fig. 15b) and sea level rise (*S*2) of a given year, model cross-

[1] Water levels are relative to the sea level in 2000.

shore profile of a previous year, and a calibration coefficient unique to each observed cliff retreat rate (192 cases, Figure 15a). In addition, runs using Trenhaile-Lite and Energy-Flux models were initiated with a 2012 cross-shore profile obtained during the model calibration. In total, 768 prediction runs were conducted considering four models and 192 observed cliff retreat rates.

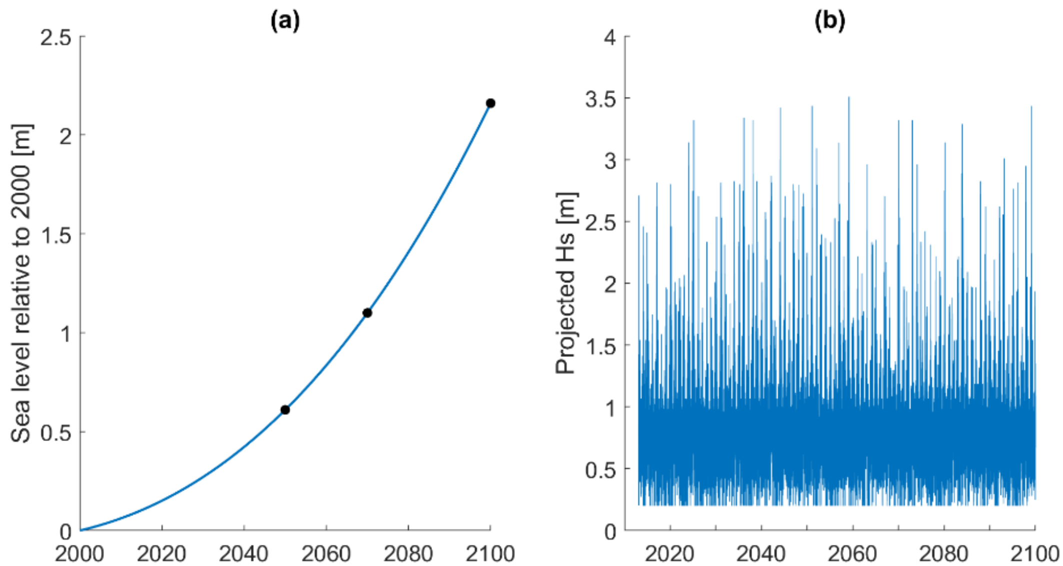

Figure 16. (a) Sea level rise scenario and (b) projected significant wave height (Hs) between 2012-2100 used for model runs.

Table 3. Parameter values for runs using the modified Bruun model

Active profile length (*L*)	400 m
Cliff height (*B*)	17.5 m
Closure depth	8 m
Proportion of sediment eroded that is sufficient coarse to remain within the equilibrium profile (*P*, from Young et al., 2010)	0.9

6.4 Model prediction output

For runs from all four models, modeled cliff retreat rates increased through time as sea level rise rates accelerated (Figure 17 and Table 4). The modified Bruun model predicted the highest cliff retreat with a median of 36.9 m in 2100 (relative to 2012 cliff base position), as opposed to 20.7 m (modified SCAPE), 17.5 m (Trenahile-Lite), and 16.5 m (Energy-Flux). Compared to other models, the modified SCAPE model predicted the largest range of 2100 cliff retreat at 1.8-51 m. Trenhaile-Lite and Energy-Flux models predicted the least cliff retreat on average with the 25th - 75th percentile ranges of 14.4-23.0 m and 13.6-21.5 m in 2100, respectively. With all model results combined, the 25th percentile, median, and 75th percentile cliff retreat in 2100 was predicted to be 15.4 m, 21.8 m, and 33.9 m, respectively.

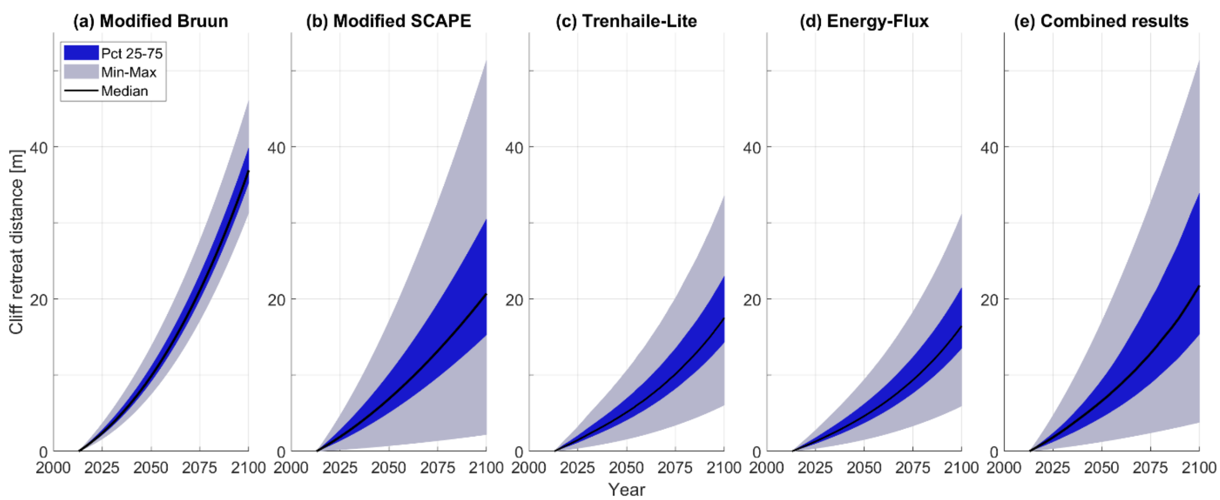

Figure 17. Median (black), minimum and maximum (gray), and 25th and 75th percentile (blue) results of simulated cliff retreat predicted by (a) modified Brunn, (b) modified SCAPE, (c) Trenhaile-Lite, and (d) Energy-Flux models. (e) Results combining all model outputs.

Table 4. Median, minimum, maximum, and 25th and 75th percentile values of simulated cliff retreat in 2100 predicted by modified Brunn, modified SCAPE, Trenhaile-Lite, and Energy-Flux models, and results combining all model outputs.

	Modified Bruun	**Modified SCAPE**	**Trenhaile-Lite**	**Energy-Flux**	**All models combined**
Minimum (m)	31.3	1.8	5.8	5.7	1.8
25th percentile (m)	35.3	15.3	14.4	13.6	15.4
Median (m)	36.9	20.7	17.5	16.5	21.8
75th percentile (m)	39.8	30.5	23.0	21.5	33.9
Maximum (m)	46.1	51.4	33.6	31.2	51.4

Scenarios with retreat of about 10 m or more intersect with the proposed project at the Solamar and Carlsbad Boulevard roundabout and a recreational trail in the southern portion of the forecast area (Figure 18). 10 m of retreat is lower than the 25th percentile for all four model outcomes (Table 4). Present infrastructure in northern end of the forecast area becomes threatened under retreat scenarios with about 20 m of retreat, which is approximately the median retreat predicted from combined model. Observed cliff retreat rate between 1998-2020 ranged up to 0.18 m/yr (Figure 15a), suggesting portions of the forecast area could exceed 10 m of retreat by 2100 even without considering the forecasted accelerated sea level rise. In addition, the cliff base retreat in the Solamar area has exceeded the cliff top retreat in many areas recently, indicating cliff steeping and increasing cliff top instability (Figure 10e). None of the models used have been validated with observations and caution should be used when interpreting the model outcomes.

Figure 18. Map of the forecast area showing proposed road alignment and zones of cliff retreat relative to the 2020 cliff top position.

7.0 References

Ashton, A.D., Walkden, M.J., & Dickson, M.E. (2011). Equilibrium responses of cliffed coasts to changes in the rate of sea level rise *Marine Geology* 284(1), 217–229.

Barnard, P.L., Erikson, L.H., Foxgrover, A.C., Limber, P.W., O'Neill, A.C., & Vitousek, S. (2018). Coastal Storm Modeling System (CoSMoS) for Southern California, v3.0, Phase 2 (ver. 1g, May 2018): U.S. Geological Survey data release.

Battjes, J.A. (1975). Surf similarity. In Coastal Engineering 1974 (pp. 466-480).

Benumof, B.T., & Griggs, G.B. (1999). The dependence of seacliff erosion rates on cliff material properties and physical processes: San Diego County, California. *Shore & Beach*, 67(4), 29-41.

Birkemeier, W., Flick R.E, Sterrett, K., Guza R.T., Seymour, R.J., O'Reilly, W.C., & Thomas, J. (2012). West Coast Closure Depth and SCBPS Beach Surveys. Presented by W.C. O'Reilly to the California Sediment Management Working Group on 11/14/2012 in San Francisco, California.

Bray, M.J., & Hooke, J.M. (1997). Prediction of soft-cliff retreat with accelerating SLR. *Journal of Coastal Research* 13, 453–467.

City of Carlsbad Sea Level Rise Vulnerability Assessment. December 2017.

Hapke, C., Reid, D., & Borrelli, M. (2008). A GIS Compilation of Vector Cliff Edges and Associated Cliff Erosion Data for the California Coast 2007, revised 2008.

Hapke, C.J., Reid, D., & Richmond, B. (2009). Rates and trends of coastal change in California and the regional behavior of the beach and cliff system. *Journal of Coastal Research*, 25(3), 603-615.

Hegermiller, C.A., Erikson, L.H., & Barnard, P. (2016). Nearshore waves in southern California: hindcast, and modeled historical and 21st-century projected time series. U.S. Geological Survey.

Limber, P.W., Barnard, P.L., Vitousek, S., & Erickson, L.H. (2018). A model ensemble for projecting multidecadal coastal cliff retreat during the 21st century. *Journal of Geophysical Research: Earth Surface* 123, 1566-1589.

Katz, O., Reches, Z., & Roegiers, J.C. (2000). Evaluation of mechanical rock properties using a Schmidt hammer. *International Journal of Rock Mechanics and Mining Sciences* 37, 723–728.

Moore, L.J., Benumof, B.T., & Griggs, G.B. (1999). Coastal erosion hazards in Santa Cruz and San Diego Counties, California. *Journal of Coastal Research*, 121-139.

OPC, 2018. State of California Sea Level Rise Guidance, 2018 Update. Ocean Protection Council: Sacramento, CA, USA, 84.

O'Reilly, W.C., Olfe, C., Thomas, J., Seymour, R.J., & Guza, R.T. (2016). The California coastal wave monitoring and prediction system. *Coastal Engineering*, 116, 118–132.

Sibson, R. (1981). "A brief description of natural neighbor interpolation (Chapter 2)". In V. Barnett (ed.). Interpreting Multivariate Data. Chichester: John Wiley, 21–36

Swirad, Z.M., & Young, A.P. (2021). Automating coastal cliff erosion measurements from large-area LiDAR datasets in California, USA. *Geomorphology, 389 (107799), 15.*

Swirad, Z.M., & Young, A.P. (In Review) CliffDelineaTool v1.1.0: an algorithm for identifying coastal cliff base and top positions, *Geoscience Model Development*.

Trenhaile, A. S. (2000_. Modeling the development of wave-cut shore platforms. *Marine Geology* 166(1), 163–178.

Walkden, M., & Dickson, M. (2008). Equilibrium erosion of soft rock shores with a shallow or absent beach under increased SLR. *Marine Geology* 251(1), 75-84.

Young, A.P., & Ashford, S.A. (2006). Application of airborne LIDAR for seacliff volumetric change and beach-sediment budget contributions. *Journal of Coastal Research, 22*(2), 307-318.

Young, A.P., Raymond, J.H., Sorenson, J., Johnstone, E.A., Driscoll, N.W., Flick, R.E., & Guza, R.T. (2010). Coarse sediment yields from seacliff erosion in the Oceanside Littoral cell. *Journal of Coastal Research* 26 (3), 580-585.

Young, A.P., Guza, R.T., Flick, R.E., O'Reilly, W.C., & Gutierrez, R. (2009a). Rain, waves, and short-term evolution of composite seacliffs in southern California. *Marine Geology, 267*(1-2), 1-7.

Young, A.P., Flick, R.E., Gutierrez, R., & Guza, R.T. (2009b). Comparison of short-term seacliff retreat measurement methods in Del Mar, California. *Geomorphology*, 112(3-4), 318-323.

Young, A.P., Guza, R.T., O'Reilly, W.C., Burvingt, O., & Flick, R.E. (2016), Observations of coastal cliff base waves, sand levels, and cliff top shaking, *Earth Surface Processes and Landforms*, *41, 1564– 1573*.

Young, A.P. (2018), Decadal-scale coastal cliff retreat in southern and central California. *Geomorphology, 300, 164-175.*

Young, A.P., Guza, R.T., Matsumoto, H., Merrifield, M.A., O'Reilly, W.C., & Swirad, Z.M. (2021). Three years of weekly observations of coastal cliff erosion by waves and rainfall. *Geomorphology, 375*.